



**HAL**  
open science

## SOFC 5 kWe CHP field unit: effect of the methane dilution

Massimo Santarelli, Marcello Gariglio, Ferrante de Benedictis, Francesco Delloro, Michele Cali', Gianmichele Orsello

► **To cite this version:**

Massimo Santarelli, Marcello Gariglio, Ferrante de Benedictis, Francesco Delloro, Michele Cali', et al.. SOFC 5 kWe CHP field unit: effect of the methane dilution. *Fuel Cells*, 2010, 10 (3), pp.453. 10.1002/face.200900096 . hal-00552357

**HAL Id: hal-00552357**

**<https://hal.science/hal-00552357>**

Submitted on 6 Jan 2011

**HAL** is a multi-disciplinary open access archive for the deposit and dissemination of scientific research documents, whether they are published or not. The documents may come from teaching and research institutions in France or abroad, or from public or private research centers.

L'archive ouverte pluridisciplinaire **HAL**, est destinée au dépôt et à la diffusion de documents scientifiques de niveau recherche, publiés ou non, émanant des établissements d'enseignement et de recherche français ou étrangers, des laboratoires publics ou privés.



### SOFC 5 kWe CHP field unit: effect of the methane dilution

Journal:	<i>Fuel Cells</i>
Manuscript ID:	face.200900096.R1
Wiley - Manuscript type:	Original Research Paper
Date Submitted by the Author:	12-Dec-2009
Complete List of Authors:	Santarelli, Massimo; Politecnico di Torino, Energetics Gariglio, Marcello; Politecnico di Torino, Energetics De Benedictis, Ferrante; TurboCare spa Delloro, Francesco; Politecnico di Torino, Energetics Cali', Michele; Politecnico di Torino, Energetics Orsello, Gianmichele; TurboCare spa
Keywords:	SOFC, real operating stack, diluted fuel, factorial design, fuel distribution



## SOFC 5 kW<sub>e</sub> CHP field unit: effect of the methane dilution

Santarelli<sup>1</sup> M., Gariglio<sup>1</sup> M., De Benedictis<sup>1,2</sup> F., Delloro F<sup>1</sup>, Cali<sup>1</sup> M., Orsello<sup>2</sup> G.

<sup>1</sup>Dipartimento di Energetica. Politecnico di Torino. Corso Duca degli Abruzzi 24, 10129 Torino (Italy)

<sup>2</sup>TurboCare S.p.A., Corso Romania 661, 10156 Torino (Italy)

e.mail: [marcello.gariglio@polito.it](mailto:marcello.gariglio@polito.it), [ferrante.debenedictis@siemens.com](mailto:ferrante.debenedictis@siemens.com), [francesco.delloro@polito.it](mailto:francesco.delloro@polito.it),

[massimo.santarelli@polito.it](mailto:massimo.santarelli@polito.it), [michele.cali@polito.it](mailto:michele.cali@polito.it), [Gianmichele.Orsello@siemens.com](mailto:Gianmichele.Orsello@siemens.com).

### Abstract

TurboCare and Politecnico di Torino (Italy), have installed a SOFC laboratory in order to analyze the operation of two SOFC generators (Project EOS-100 kW and EBE-5 kW) built by Siemens Power Corporation (SPC). In the EBE project the installation of the SFC5 SOFC generator (3.5 kW<sub>e</sub> and 3 kW<sub>th</sub>) was carried out. To date, it has operated in the workshop canteen for more than 15,984 hours with very high reliability.

The real stack is a complex system not installed in a Lab environment, and has several effects of not-homogeneity in terms of electrochemical response to fuel or air management modifications. Moreover, many of the parameters of the stack are not directly measurable, and have to be inferred by indirect measurements.

In this paper, the analysis of the not homogeneous behaviour of the different segments of the complete stack is performed, through an experimental session using a not conventional fuel.

The obtained data have been analyzed using the ANOVA for every dependent variable and a non-linear regression model for the voltage. Those models were used to evaluate the effect of the fuel modification on the local fuel utilization in different sectors of the stack.

**Keywords:** SOFC, real stack, diluted fuel, factorial design.

## 1. Introduction

TurboCare S.p.A. (TC) and Politecnico di Torino, both located in Torino (Italy), have installed a SOFC laboratory in order to analyze the operation, in a cogenerative configuration, of two generators built by Siemens Power Corporation (SPC): the SOFC CHP100 and the 5 kW Alpha6 Generator.

Some experimental and modeling activities were performed during the four years of operations, involving some aspect of installation and operation in a real industrial environment.

The EBE project (Energia a Basse Emissioni) concern the Alpha6 Generator (SFC5 alpha6), providing 3.5 kW<sub>e</sub> of electric energy delivered to the grid and about 3 kW<sub>th</sub> of thermal energy supplied to the TC canteen. The generator was installed in April 2006, and at present it runs from more than 15,900 hours and has delivered to the grid about 47.7 MWh. The initiative is highly innovative because in Italy there are not plants for micro-cogeneration on 1-5 kW scale based on solid oxide fuel cell. This technology is devoted to small electrical generation for civil use (big flat, small office, house).

The Politecnico di Torino developed several activities in the laboratory [1-6]. In [7] a sensitivity analysis of voltages against fuel utilization and generator temperature, and an optimization of the system by regression model, has been proposed, while another experimental campaign was devoted to study the effect of air distribution inside the stack. Then an experimental campaign has been carried out in order to analyze the effect of

1  
2  
3  
4 changing the most important operating parameters (generator temperature, fuel utilization  
5 and current), in order to obtain the generator polarization model [8].  
6  
7

8  
9 The real stack is a complex system not installed in a Lab environment, and has several  
10 effects of not-homogeneity in terms of electrochemical response to fuel or air management  
11 modifications. Moreover, many of the parameters of the stack are not directly measurable,  
12 and have to be inferred by indirect measurements.  
13  
14

15  
16 Compared to studies on a single cell, where the temperature can be easily controlled to  
17 impose homogeneity on the cell surface, on a large SOFC generator we have different  
18 temperature profiles on cells placed in different segments of the stack. In particular, it is  
19 possible to observe that for the segments close to the in-stack reformer the temperature is  
20 lower than the other part of the generator (due to the cooling effect of the steam reforming  
21 reaction occurring into the reformer section). Another cause of this not homogeneity of  
22 temperature distribution is due to the fluid-dynamic of the reactant flows inside the stack  
23 (air and fuel) [7].  
24  
25  
26  
27  
28  
29  
30  
31  
32  
33  
34  
35  
36

37 Moreover, a further problem on the characterization of large systems is the difference of  
38 pedigree and degradation level on the single cells that compose the stack [9].  
39  
40

41  
42 Biogas fuel feeding present an attractive option among emerging applications for fuel cells,  
43 especially for solid oxide fuel cell. Usually, biogas is a local resource and residues from  
44 farms and municipalities typically represent small fuel sources (in the range of 5-100 kW)  
45 suitable for fuel cell system.  
46  
47  
48  
49

50  
51 Several groups have studied SOFC fuel flexibility in recent years using theoretical analysis  
52 or simulation work [10-14]. A 1 kW<sub>el</sub> SOFC unit from Sulzer HEXIS, Switzerland, was  
53 successfully operated on farm biogas in Switzerland for one year [15,16]. Fuel Cell  
54  
55  
56  
57  
58  
59  
60

1  
2  
3  
4 Technologies (FCT) from Canada demonstrate 5 kW<sub>el</sub> SOFC units also for biogas  
5 application [17].  
6  
7

8  
9 In this paper, the analysis of the not homogeneous behaviour of the different segments of  
10 the complete Siemens 5 kW alpha6 stack is performed, through an experimental session  
11 using a not conventional fuel. The scheduled tests have been carried out in April 2008. This  
12 is the first experimental campaign using a non conventional fuel and it yielded interesting  
13 results about fuel distribution inside the stack, which are presented in section 8.  
14  
15  
16  
17  
18  
19

## 20 21 22 **2. System description** 23

24 The Alpha6 Generator utilizes the commercial prototype air electrode supported cells (22  
25 mm diameter, 75 cm active length, 384 cm<sup>2</sup> active area). The generator is fed with natural  
26 gas from the grid distribution. In Figure 1 the picture representing the Alpha6 Generator  
27 test site in TurboCare is shown.  
28  
29  
30  
31  
32  
33  
34

### 35 36 **Figure 1. Picture of the Alpha6 Generator test site in TurboCare (Torino, 37 Italy)** 38

39  
40 The upper level of system hierarchy after the single cell is the sector, which consists of a  
41 22-cell array arranged as 11 cells in electrical series by 2 cells in electrical parallel; 4  
42 sectors are aligned side by side, interconnected in serpentine (for a total of 88 single tubes).  
43  
44 In Figure 2 a simplified scheme of the Balance of Plant of the 5 kW<sub>e</sub> Alpha6 Generator is  
45 shown.  
46  
47  
48  
49  
50  
51  
52

### 53 54 **Figure 2. Simplified scheme of the Balance of Plant of the 5 kW<sub>e</sub> Alpha6 55 Generator** 56 57 58 59 60

1  
2  
3  
4 The SOFC module includes an in-stack fuel reformer which is placed in the middle of the  
5 stack. This reformer uses heat from the SOFC operation to provide the energy needed to  
6 convert the hydrocarbon fuel into hydrogen and carbon monoxide. The SOFC module also  
7 includes an internal air recuperator to recover heat allowing higher operational efficiency.  
8

9  
10  
11 The function of the ECS (Electronic Control System) is to monitor all the components and  
12 sensors (current, voltage, temperature, etc.) in addition to load demands from the inverter.  
13

14  
15  
16 In the following, some results obtained in different previous experimental campaigns for  
17 sector voltages, system AC power and efficiency are presented [8]. Experimental data have  
18 been analyzed using the design of experiment approach, which allows to apply analysis of  
19 variance (ANOVA) [18] and to obtain a regression model for the dependent variables. All  
20 the results presented in this section derive from the analysis of the regression models.  
21

22  
23  
24 In Figure 3 the cell polarization for sector A and sector B, at fixed average stack  
25 temperature ( $T_{\text{gen}}=960^{\circ}\text{C}$ ), and as a function of fuel utilization (FU), are shown.  
26  
27

### 28 **Figure 3. Polarization model for sector A and B, function of FU**

29  
30  
31 Voltages have an expected behavior when varying fuel utilization parameter. In both  
32 sectors it is evident that voltage sensitivity to FU is higher at high FU values: at high FU, a  
33 variation of FU corresponds to a larger variation in the cell voltage, with respect to the low  
34 FU case. In sector B it is also possible to note larger fuel sensitivity at high current density.  
35

36  
37  
38 In Figure 4, AC power output of the system for different  $T_{\text{gen}}$  and FU conditions is shown.  
39  
40  
41

#### Figure 4. AC power model, function of current density, $T_{\text{gen}}$ and FU

AC electric power has an expected behavior: an increase in generator average temperature causes an increase in AC power, and this fact is mainly due to a reduction of ohmic losses. The higher temperature causes also a reduction of the activation overvoltages. Besides, an increase in fuel utilization causes a reduction of the AC power. This behaviour is mainly due to Nernst voltage dependence on anodic partial pressures.

In Figure 5 the behavior of the global efficiency, with variations of  $T_{\text{gen}}$  and FU, is shown.

#### Figure 5. Global efficiency model, function of current density, $T_{\text{gen}}$ and FU

With lower generator average temperature, it is observed a slightly higher global efficiency. This fact can be interpreted considering that the global efficiency is the sum of the AC electrical efficiency and of the thermal efficiency. In this case, the decrease in AC efficiency, due to larger ohmic losses, is balanced by the increase of thermal efficiency. The latter is linked to a higher air flow (needed for the stack cooling because of the larger ohmic losses), which makes available a higher heat recovery.

It is interesting to analyse the variations of global efficiency with fuel utilization. It can be seen from Figure 5 that exists a value of fuel utilization, within the experimental domain, that maximizes the global efficiency. It follows directly from the observation that AC efficiency is monotonic w.r.t. FU, while thermal efficiency presents a maximum at a certain FU value. The latter is due to a balance between the effects of FU on two parameters: 1) exhaust mass flow; 2) exhaust temperature.

1  
2  
3  
4 Rising FU results in an enhancement in heat production into the stack, due to an increase in  
5  
6 irreversibilities and a reduction in the cooling effect of the fuel flow, and this causes an  
7  
8 increase of the air flow (and consequently of the exhaust flow) in order to control the  
9  
10 average stack temperature; but the prevailing effect is a reduction of the exhaust  
11  
12 temperature (due to the reduction of the heat from the post-combustion), causing a  
13  
14 reduction of the heat recovered. Reducing FU the increase of the exhaust temperature  
15  
16 becomes important, but at the same time the higher efficiency of the stack translates in a  
17  
18 reduction of the heat from irreversibility, and a decrease of the air (and exhaust) mass flow.  
19  
20 Therefore, there is a value of the FU where a balance of the two effects occurs, causing a  
21  
22 maximization of the thermal recovery and as consequence a maximization of the global  
23  
24 efficiency.  
25  
26  
27  
28  
29

30 An important feature of SFC 5 alpha6 is the possibility to control the air flowing to every  
31  
32 single sector of the stack. The air management system consists in a series of manual valves  
33  
34 that allow to control the air flow through the single sectors of the stack. An experimental  
35  
36 campaign has been carried out in order to evaluate the influence of the air management  
37  
38 system on the system performance and to find the optimized configuration [7]. After this  
39  
40 experimental campaign, every other experimental test has been performed with the  
41  
42 optimized configuration of air management system.  
43  
44  
45  
46  
47  
48

### 49 **3. Description of the experimental session**

50  
51  
52  
53  
54  
55  
56  
57  
58  
59  
60

1  
2  
3  
4 The scheduled tests have been carried out in April 2008, with the aim to characterize the  
5 system with different fuel compositions, different loads (current) and generator setup  
6 (average) temperature.  
7  
8

9  
10  
11 Besides, we wanted to demonstrate the possibility to operate the system when fed with a  
12 fuel with low LHV. This fuel is obtained introducing in the main natural gas stream a flow  
13 of NHmix (5% of Hydrogen in Nitrogen). In this way a methane dilution is achieved. In the  
14 following we will refer to this diluted mixture as “diluted fuel” (see Table 1). **The choice to**  
15 **use NHmix was linked to very practical reasons: this mixture is used during the start**  
16 **up and shut down of the stack, and all the connections with the stack are already**  
17 **placed in the BoP.**  
18  
19  
20  
21  
22  
23  
24  
25  
26  
27

28 Moreover, the variation of the Fuel Utilization factor allowed to perform a sensitivity  
29 analysis of voltages against fuel utilization. In fact, as already discussed and performed in  
30 [22], the fuel sensitivity tests can be used as a diagnostic tool to investigate the fuel  
31 distribution on a large SOFC stack. As discussed below, an interesting result has been  
32 obtained: when the system is fed with this diluted fuel, a better fuel distribution inside the  
33 stack has been obtained, if compared to simple natural gas feeding.  
34  
35  
36  
37  
38  
39  
40  
41

42 The test session has been planned following a factorial experimental design, where some  
43 controllable variables (factors) are varied among discrete possible values or "levels"  
44 (usually two: low and high value); the complete experiment takes on all the possible  
45 combinations of these levels across all those factors [18], allowing the analysis of the main  
46 and interaction effects of all the factors on the dependent variables of the system.  
47  
48  
49  
50  
51  
52  
53  
54  
55  
56  
57  
58  
59  
60

1  
2  
3  
4 to evaluate the main and interaction effect of the three factors (generator average  
5 temperature ( $T_{\text{gen}}$ ), stack current (I) and fuel composition – see Table 1) on several  
6  
7 dependent variables expressing the performance of the generator. The design of experiment  
8  
9 adopted is a simple  $2^3$  factorial design (Figure 6), which allows to obtain first order  
10  
11 regression model of the dependent variables as functions of the independent factors. The  
12  
13 range of variation of each factor has been imposed in agreement with TurboCare, in order  
14  
15 to avoid malfunction of the generator.  
16  
17  
18  
19  
20  
21  
22  
23

### Figure 6. $2^3$ factorial design

#### Table 1. Values of the factors ion the factorial design

24  
25  
26  
27  
28  
29  
30 In Table 2 the fuels composition in the two considered fuel options (natural gas and diluted  
31  
32 fuel) are shown.  
33  
34  
35

#### Table 2. Fuels composition of the experimental session

36  
37  
38  
39 **It has to be specified that the thermal balance of the complete stack can be influenced**  
40  
41 **by the chemical reactions occurring in the “in-stack” reformer, where different**  
42  
43 **reactions (exothermic and endothermic) take place whether fuels of different**  
44  
45 **composition are sent to the reformer unit. The different enthalpies of reaction could**  
46  
47 **determine a modification of the thermal balance, and thus of the average stack**  
48  
49 **temperature: as an example, since the steam-reforming of a ethanol stream is**  
50  
51 **somewhat less endothermic than the methane one, a higher stack temperature could**  
52  
53 **be observed. Anyway, in these SOFC systems the stack temperature can be considered**  
54  
55  
56  
57  
58  
59  
60

1  
2  
3  
4 as a independent variable (thus not depending on the reactions occurring in the  
5 reformer), since the air stoichs is the parameter managing the stack temperature: we  
6 could impose a air stoichs in such a way to keep the stack temperature constant.  
7  
8  
9  
10  
11  
12  
13  
14  
15  
16  
17  
18  
19  
20  
21  
22  
23  
24  
25  
26  
27  
28  
29  
30  
31  
32  
33  
34  
35  
36  
37  
38  
39  
40  
41  
42  
43  
44  
45  
46  
47  
48  
49  
50  
51  
52  
53  
54  
55  
56  
57  
58  
59  
60

as a independent variable (thus not depending on the reactions occurring in the reformer), since the air stoichs is the parameter managing the stack temperature: we could impose a air stoichs in such a way to keep the stack temperature constant. When a less endothermic reforming reaction is taking place, an increase of the the stack temperature is avoided augmenting the air flow into the stack in order to cool down the Generator.

#### 4. ASR data analysis

A preliminary analysis on the sector voltage data consisted in the evaluation of the Area Specific Resistance (ASR). ASR is an index of the slope of the polarization curve that can be used as an indicator of the performance of the cells. It is defined by  $dV/di$  at 0.7 V and is determined from the slope of the best fitting line over the measured data within the interval 0.65 – 0.75 V. In our case it is not possible to evaluate the ASR with the given definition because the tests have been designed with only two current levels, thus it is evaluated as:

$$ASR = \left| \frac{V_1 - V_2}{i_1 - i_2} \right| \quad (1)$$

In Figure 7 the influence of generator setup temperature on sectors ASR with different fuel is shown.

**Figure 7. ASR distribution function of fuel composition and generator average temperature**

1  
2  
3  
4 In both cases an increase of the generator average temperature causes a reduction of the  
5 ASR. All the overvoltages of the polarization curve are influenced by the generator average  
6 temperature but the ohmic overvoltage is the most influenced by this parameter, and it  
7 decreases with an increase of the generator average temperature. The variations of ASR  
8 with temperature is more evident on sectors B.

9  
10  
11 From the figure it is evident a different slope for the sectors. This is due to higher ohmic  
12 losses in sector B, caused probably by the partial interconnection detachment and a  
13 consequent increase in contact resistance.

14  
15  
16 In Figure 8 the average ASR comparison for different feeding fuel is shown.

### 17 18 19 20 21 22 23 24 25 26 27 **Figure 8. ASR function of the fuel composition**

28  
29  
30 When the system is fed with diluted gas, the ASR of each sector decreases. This behaviour  
31 cannot be explained with a temperature effect (on the contrary: the diluted fuel causes even  
32 a decrease of the local temperature); therefore, this positive effect can be linked probably to  
33 a fluid dynamic effect, which is an apparent better fuel distribution inside the stack. This  
34 effect will be analysed and explained later in section 8.

## 35 36 37 38 39 40 41 42 43 **5. Regression model**

44  
45  
46 This experimental campaign has been carried out following the factorial design in Figure 2,  
47 in order to apply the ANOVA model and to study the effect of each parameter  
48 independently. Nevertheless, the system has not been able to keep sufficiently stable  
49 operation conditions in terms of fuel utilization, a parameter with an important influence on  
50 the voltage and which has not been considered as a factor in the design of experiment. This

1  
2  
3  
4 inconvenience is caused by the control system. In fact, SFC5 is a pre-commercial prototype  
5  
6 and the actual control system is designed for equipment safety purposes and is not suitable  
7  
8 for thorough experimentation. To overcome this problem and to allow more accurate  
9  
10 testing sessions, it would be necessary to develop a dedicated control system. Because of  
11  
12 the difficulties explained, we couldn't rely on the ANOVA analysis for our data, and  
13  
14 decided to perform a non-linear fit on the voltages, as functions of FU, generator average  
15  
16 temperature and current density. We treated separately the data for different fuel  
17  
18 conditions: so different regressions model of the voltage for natural gas and diluted gas,  
19  
20 namely  $V_{NG}$  and  $V_{SG}$ , were obtained.  
21  
22  
23  
24

25  
26 Due to the complexity of the system, we decided to not apply a typical polarization model.  
27  
28 In fact in a large stack, like the Alpha6 Generator, there are some factors that cannot be  
29  
30 perfectly under control, i.e. local fuel distribution or local temperature. For this reason we  
31  
32 decided to adopt a more empirical model, although inspired by the standard analytical  
33  
34 polarization model for single cells. In particular, we considered Nernst, ohmic, activation  
35  
36 and concentration (i.e. depletion of reactants) overvoltages. Only the effect of diffusive  
37  
38 transport in the porous anode and cathode has not been considered in the model because, in  
39  
40 the operating conditions (low-medium current densities), it resulted negligible compared to  
41  
42 the others.  
43  
44  
45

46  
47 The classical expression for reversible voltage is [19]:  
48  
49  
50  
51

$$V_{rev} = -\frac{\Delta G^R(T)}{2F} + \frac{RT}{2F} \log \left( \frac{P_{H_2} P_{O_2}^{0.5}}{P_{H_2O}} \right) \quad (2)$$

52  
53  
54  
55  
56  
57  
58  
59  
60

The partial pressure dependence of this expression can be rewritten in terms of Fuel Utilization factor and air stoichs, both measured by the control system [22]:

$$E = E_0 - \frac{R \cdot T}{2 \cdot F} \cdot \ln \left[ \frac{FU \cdot \left( \frac{\lambda}{\sigma_{O_2}} - FU \right)^{0.5}}{(1-FU) \cdot (\lambda - FU)^{0.5}} \right] \quad (3)$$

As a further simplification, temperature dependence is neglected due to the not significant effect linked to the low temperature modification in the tests, and a simple  $\log(1-FU)$  term is used to take into account the dependence on the partial pressures of gases.

Concerning Ohmic overvoltage, it is linear with respect to the current, and a simplified empirical dependence on temperature has been assumed. Activation overvoltage was modeled by means of the standard Butler-Volmer expression, again neglecting temperature dependence. The following non-linear expression has been chosen for the voltages:

$$V(FU, T, i) = \underbrace{\beta_1}_{\text{Nernst}} + \underbrace{\beta_2 \log(1 - FU)}_{\text{Concentration}} + \underbrace{\beta_3 \frac{i}{\log \frac{1}{T}}}_{\text{Ohmic}} + \underbrace{\beta_4 \sinh^{-1} \left[ \frac{i}{\beta_5 FU \exp \frac{-10^5}{FU}} \right]}_{\text{Activation}} \quad (4)$$

A remark should be added about  $\beta_5$ : due to the great discrepancy of literature data regarding exchange current density for the cathode, we chose to add this fitting parameter.

The best fitting values of the parameters  $\beta_i$  have been found with the Gauss-Newton method [20]. As seen, we have very simple temperature dependence, involving only one parameter. On the other hand the FU appears in two terms and three parameters can be tuned in order to fit accurately the model to the data variations.

1  
2  
3  
4 Since the expression chosen is suggested by physical considerations but represents a  
5  
6 simplified empirical model, the  $\beta_i$  values don't have a strong physical meaning.  
7  
8

9 For the other dependent variables a linear model building procedure is adopted  
10  
11

## 12 13 14 **6. Voltage analysis** 15

16  
17 In Figure 9 the effects of current, fuel utilization and fuel composition on the sector  
18  
19 voltages obtained with the regression model are shown, and compared with the  
20  
21 experimental data.  
22

23  
24 The difference between regression model and experimental data are due to the fact that the  
25  
26 model can fix the values of independent factors (essentially, setup temperature and FU),  
27  
28 while in the real experimental session the control system is not able to maintain a constant  
29  
30 value at the desired set point but there is a tolerance in the values of setup temperature and  
31  
32 FU.  
33  
34

### 35 36 37 38 **Figure 9. Polarization regression model function of current density, FU** 39 40 **and fuel composition** 41

42  
43 Sector A shows an expected behavior. In fact, when the system is fed with diluted fuel, a  
44  
45 voltage decrease is observed, due to the dependence of the exchange current density on  
46  
47 reactant partial pressures. Also an increase in fuel utilization causes a voltage decrease.  
48

49  
50 On the other hand, sector B shows an unexpected behavior with respect to variations in the  
51  
52 feeding fuel. Here, when the system is fed with diluted fuel, the voltage is higher than with  
53  
54

1  
2  
3  
4 natural gas feeding. We will discuss this topic in the following section, with the aid of  
5  
6 sensitivity analysis.  
7

8  
9 The developed regression model operates quite well and also confirms the same  
10  
11 observation made experimentally: a different slope for sector B due to higher ohmic losses,  
12  
13 caused probably partial interconnection detachment and a consequent increase in contact  
14  
15 resistance.  
16  
17

## 20 21 **8. Fuel sensitivity and local fuel utilization estimation**

22  
23 In this paragraph the voltage sensitivity to fuel utilization and its relation with local fuel  
24  
25 utilization are presented. Before focusing on the topic, it must be observed that the FU  
26  
27 parameter is a global variable, i.e. we don't have different measurements for each sector but  
28  
29 only one for the whole stack.  
30  
31

32  
33 Sensitivity of voltage to fuel utilization ( $dV/dFU$ ) is an important variable when studying  
34  
35 solid oxide fuel cell systems. In a previous work [21-22] it has been demonstrated that the  
36  
37 sensitivity of cell voltage to fuel utilization depends on several contributions, which  
38  
39 concern the Nernstian term, the diffusion term and eventually the effect of leakages of air at  
40  
41 the anode side. At low current density the fuel utilization sensitivity is governed essentially  
42  
43 by the variation of the average Nernst voltage with FU whereas at high current density the  
44  
45 effect of diffusion and leakages become more effective. Moreover, it has been shown that  
46  
47 there is a direct relationship between the voltage sensitivity to fuel utilization and the local  
48  
49 value of the fuel utilization in operation, and therefore to the fuel distribution inside the  
50  
51 stack.  
52  
53  
54  
55  
56  
57  
58  
59  
60

1  
2  
3  
4 Considering the obtained regression model of the sector voltage, it is possible to calculate  
5 analytical expressions for the derivative ( $dV/dFU$ ), as a function of Fuel Utilization. The  
6 local fuel utilization of a sector can be estimated by comparing the measured fuel  
7 sensitivity value (measured value  $F^0$ ) with the expression calculated from the voltage  
8 regression model. In other words, we look for a solution of:  
9  
10  
11  
12  
13  
14  
15  
16  
17  
18  
19  
20  
21  
22  
23  
24

$$\frac{\partial V(FU)}{\partial FU} = F^0 \quad (5)$$

25 The solution is the estimation of local FU. Note that here the only variable is FU, since  
26 temperature and current are measured and inserted into the regression model.  
27  
28  
29

30 This procedure can be performed both with natural gas and diluted fuel, therefore allowing  
31 an analysis of the fuel distribution in the stack sectors with different fuel conditions.  
32  
33  
34

35 The distribution of fuel utilization sensitivity, according to the proposed model, depends on  
36 the local temperature and on the local fuel utilization; a limit of the estimation is that the  
37 effect of the temperature is neglected in the following analysis, due to the fact that we  
38 cannot know the local temperature.  
39  
40  
41  
42  
43

44 In Figure 10 it is shown how local FU values are obtained from voltage sensitivity curves  
45 for sectors A and B.  
46  
47  
48

49 It is well known that differences between local fuel utilization values are caused by a non  
50 uniform fuel distribution among the sectors: a higher local FU means a lower fuel flow to  
51 the sector.  
52  
53  
54  
55  
56  
57  
58  
59  
60

### **Figure 10. Estimation of local values of fuel utilization through analysis of voltage sensitivity to fuel utilization**

With diluted fuel, the sensitivities are much higher than with natural gas. The evaluation of local fuel utilization in Table 3 compares two sectors in two different feeding conditions.

#### **Table 3. Estimation of local fuel utilization**

With natural gas, sector B shows a higher value of local FU, so it seems that sector B is penalized by the fuel distribution. On the other hand, when the system is fed with diluted fuel a higher mass flow reaches the anode side of the sector B. In these conditions sector A shows a local FU increase and a slight voltage decrease (Figure 4), while sector B shows an opposite behavior. It seems likely to say that with diluted fuel feeding the anodic molar flow is nearly double, and for this reason the fuel is better distributed inside the stack. Sector B, which is penalized in normal conditions because of a bad fuel distribution, can take advantage of the increased anodic flow. It is important to take into account also the role of the leakages of air to the anode side. In fact, if air leakage is large we have an important quantity of hydrogen that burns in the stack, with the consequence that it does not take part in electrochemical reactions generating current. If this occur, the effective operational local fuel utilization is higher than the expected one and sensitivity to the fuel is supposed to be very high. When feeding the system with a diluted gas, the anodic pressure increases and the leakages are reduced.

These important results are confirmed by the study of electrical behavior of the stack. In particular, it is possible to observe that when the system is fed with diluted fuel the

1  
2  
3  
4 polarization curve of the sector B is better than with natural gas, as noticed in the ASR  
5 results (Figure 8).  
6  
7  
8  
9

## 10 11 **9. Conclusions**

12  
13  
14 In the paper, the experimental campaign had the aim to demonstrate the capability of the  
15 system to run with low LHV fuel, and especially to analyse the complex effects of feeding  
16 a diluted fuel on a large stack composed of several sectors. The results can be summarized  
17 as follow:  
18  
19  
20  
21  
22

- 23  
24 • Was demonstrated the capability of SOFC stack to operate with low energy content  
25 in the fuel.  
26
- 27  
28 • The ASR of the different sectors decreases when the system is fed with diluted fuel:  
29 this behavior is caused by the better fuel distribution inside the stack (at the same  
30 condition activation overpotential decreases).  
31  
32
- 33  
34 • The ASR value of Sector B is higher than other sectors: this behavior is probably  
35 due to partial interconnection detachment that causes an increase of ohmic  
36 overvoltage .  
37  
38
- 39  
40 • A simplified not linear regression model starting from the physical expression of  
41 cell voltage was developed in order to investigate the experimental domain.  
42  
43
- 44  
45 • Sector A and sector B voltages show opposite behaviors when the system is fed  
46 with diluted fuel: sector A shows a voltage decrease while sector B shows a voltage  
47 increase.  
48  
49  
50  
51  
52  
53  
54  
55  
56  
57  
58  
59  
60

- The analysis of the voltage sensitivity to fuel utilization can be used as a diagnostic tool to estimate the local distribution of the fuel utilization in the different sectors of the stack
- Using the diluted fuel the voltage sensitivities to fuel utilization are much higher than using natural gas.
- With natural gas feeding sector B shows a higher local FU than sector A. With diluted fuel sector A shows a local FU increase and a slight voltage decrease, while sector B shows an opposite behavior.
- With diluted fuel feeding, the fuel is better distributed inside the stack: therefore, the dilution causes an increase of the performances of the whole stack, because it determines a better internal fluid dynamic

## Acknowledgment

The authors acknowledge the Regione Piemonte and TurboCare which financially supported this work within the framework of the EOS Project (contract 470/2004).

## References

- [1] Saroglia S., Leone P., Santarelli M., Design and Development of a cogenerative system for a SOFC CHP100, Proceedings of HYSYDays 2005, 1<sup>st</sup> World Congress of Young Scientists on Hydrogen, Torino (Italy), 2005.
- [2] Cali M., Santarelli M., Leone P., Comparison of the behavior of the CHP-100 SOFC Field Unit fed by natural gas or hydrogen through a computer experimental analysis, Proceedings of World Hydrogen Technology Convention, Singapore, 2005.

- 1  
2  
3  
4 [3] Cali M., Orsello G., Santarelli M., Leone P., Experimental activity on the tubular  
5 SOFC CHP100 kWe Field Unit in Italy: factor significance, effects and regression  
6 model analysis, Proceedings of ESDA2006, 8th Biennial ASME Conference on  
7 Engineering Systems Design and Analysis, Torino (Italy), July 2006.  
8  
9  
10  
11  
12  
13  
14 [4] Santarelli M., Leone P., Cali M., De Benedictis F., Experimental Activity on the  
15 Tubular SOFC CHP100 Generator in Italy: Regression Models Analysis and  
16 Optimization, Proceedings of Lucerne Fuel Cell Forum 2006, Lucerne (Switzerland),  
17 July 2006.  
18  
19  
20  
21  
22  
23  
24 [5] Santarelli M., Leone P., Gariglio M., Cali M., Spinelli P., Orsello G., De Benedictis  
25 F., Experimental Analysis of the Polarization Effects at Variable Local Temperature  
26 and Fuel Consumption in a 100 kWe SOFC Stack, ECS Transaction, Vol. 5 (1), 2007.  
27  
28  
29  
30  
31 [6] Gariglio M., De Benedictis F., Santarelli M., Analysis of the cooling transient of a  
32 large SOFC generator, Proceedings of HYSYDays 2007, 2<sup>nd</sup> World Congress of  
33 Young Scientists on Hydrogen, Torino (Italy), 2007.  
34  
35  
36  
37  
38 [7] Gariglio M., Santarelli M., De Benedictis F., Cali M., Orsello G., Disegna G.,  
39 Regression models analysis and optimization of a SOFC SFC 5 kWe Field Unit,  
40 Proceedings of Fuel Cell Seminar 2007, 16-20 October 2007, San Antonio (US),  
41 2007.  
42  
43  
44  
45  
46  
47 [8] Santarelli M., Gariglio M., De Benedictis F., Cali M., Disegna G., Orsello G.,  
48 Experimental Model of a 5 kW Tubular SOFC System Operating in the canteen of a  
49 workshop, Poster presentation, Fuel cell forum 2008, Lucerne 30 June – 4 July 2008  
50  
51  
52  
53  
54 [9] Anil V.V., A model for solid oxide fuel cell (SOFC) stack degradation, Journal of  
55 Power Sources, Vol. 172, pp.713-724, 2007  
56  
57  
58  
59  
60

- 1  
2  
3  
4  
5 [10] Yi Y., Rao A. D., Brouwer J., Samuelsen S., Fuel flexibility study of an integrated 25  
6 kW SOFC reformer system, *Journal of Power Sources*, Vol. 144, pp.67-76, 2005  
7  
8  
9 [11] Marsano F., Magistri L., Bozzolo M., Tarnowsky O., Influence of fuel composition  
10 on Solide Oxide Fuel Cell hybrid system layout and performance, *ASME Turbo Expo*  
11 *GT2004-53853*, Vienna, Austria.  
12  
13  
14  
15 [12] Eguki K., Kojo H., Takeguchi T., Sasaki K., Fuel flexibility in power generation by  
16 solid oxide fuel cell, *Solid State Ionics*, Vol. 152-153, pp. 411-416, 2002  
17  
18  
19 [13] Douvartzides S.L., Coutelieris F.A., Demin A.K., Tsiakaras P.E., Fuel options for  
20 solid oxide fuel cell: a thermodynamic analysis, *AIChE J.*, Vol. 49 (1), pp. 248-257,  
21 2003  
22  
23  
24  
25  
26  
27 [14] Van Herle J., Maréchal F., Leuenberger S., Favrat D., Energy balance model of a  
28 SOFC cogenerator operated with biogas, *Journal of power sources*, Vol. 118, pp. 375-  
29 383, 2003  
30  
31  
32  
33  
34 [15] Van Herle J., Membrez Y., Bucheli O., Biogas as a fuel source for SOFC co-  
35 generators, *Journal of power sources*, Vol.127, pp. 300-312, 2004  
36  
37  
38  
39 [16] Jenne M., Zahringer T., Schuler A., Piskay G., Moos D., Sulzer HEXIS SOFC system  
40 for biogas and heating oil, in: U. Bossel (Ed.), *Proceedings of the Fifth European*  
41 *Solid Oxide Fuel Cell Forum*, Lucerne, Switzerland, European Forum Secretariat, CH  
42 5442-Oberrohrdorf, Switzerland, July 2002, pp. 460-466  
43  
44  
45  
46  
47  
48 [17] <http://www.fct.ca>, <http://www.fuelcelltechnologies.com>  
49  
50  
51 [18] Montgomery D.C., *Design and analysis of experiment*, *Wiley and sons*, 2004.  
52  
53  
54 [19] Singhal S., Kendal K., *High temperature solid oxide fuel cell: fundamentals, design*  
55 *and applications*, Elsevier, 2003  
56  
57  
58  
59  
60

- 1  
2  
3  
4 [20] James V. Beck, Kenneth J. Arnold, *Parameter estimation in engineering and science*,  
5  
6 John Wiley and sons, 1997  
7  
8  
9 [21] Goplan S., Di Giuseppe G., Fuel sensitivity test in tubular solid oxide fuel cells,  
10  
11 Journal of Power Sources, Vol. 125, pp. 183-188, 2004.  
12  
13  
14 [22] Santarelli M., Leone P., Calì M., Orsello G., Experimental evaluation of the  
15  
16 sensitivity to fuel utilization and air management on a 100kW SOFC system, Journal  
17  
18 of Power Sources, Vol. 171, pp. 155-168, 2007  
19  
20  
21  
22  
23  
24  
25  
26  
27  
28  
29  
30  
31  
32  
33  
34  
35  
36  
37  
38  
39  
40  
41  
42  
43  
44  
45  
46  
47  
48  
49  
50  
51  
52  
53  
54  
55  
56  
57  
58  
59  
60

**FIGURE CAPTIONS**

Figure 1. Picture of the Alpha6 Generator test site in TurboCare (Torino, Italy)

Figure 2. Simplified scheme of the Balance of Plant of the 5 kW<sub>e</sub> Alpha6 Generator

Figure 3. Polarization model for sector A and B, function of FU

Figure 4. AC power model, function of current density, T<sub>gen</sub> and FU

Figure 5. Global efficiency model, function of current density, T<sub>gen</sub> and FU

Figure 6. 2<sup>3</sup> factorial design

Figure 7. ASR distribution function of fuel composition and generator average temperature

Figure 8. ASR function of the fuel composition

Figure 9. Polarization regression model function of current density, FU and fuel composition

Figure 10. Estimation of local values of fuel utilization through analysis of voltage sensitivity to fuel utilization

**TABLE CAPTIONS**

Table 1. Values of the factors ion the factorial design

Table 2. Fuels composition of the experimental session

Table 3. Estimation of local fuel utilization

Table 1. Values of the factors in the factorial design

<b>Factor</b>	<b>Min</b>	<b>Max</b>
<b>Diluted fuel</b>	Natural Gas	Diluted Fuel
<b>T<sub>gen</sub> (°C)</b>	949.6	967.8
<b>I (A/cm<sup>2</sup>)</b>	0.109	0.137

Table 2. Fuels composition of the experimental session

<b>Gas composition</b>	<b><math>C_xH_y</math> (%) (hydrocarbons, mainly methane)</b>	<b><math>H_2</math> (%)</b>	<b><math>CO_2</math> (%)</b>	<b><math>N_2</math> (%)</b>
<b>Natural gas</b>	97.162	0.000	1.106	1.732
<b>Diluted fuel</b>	48.770	2.490	0.555	48.185

Table 3. Estimation of local fuel utilization

	<b>Voltage sensitivity to FU [mVcell/%FU]</b>	<b>Local FU</b>
<b>Sector A – Natural gas</b>	-1.09	0.807
<b>Sector A – Diluted fuel</b>	-3.54	0.812
<b>Sector B – Natural gas</b>	-2.73	0.861
<b>Sector B – Diluted fuel</b>	-4.09	0.746

Or Peer Review

1  
2  
3  
4  
5  
6  
7  
8  
9  
10  
11  
12  
13  
14  
15  
16  
17  
18  
19  
20  
21  
22  
23  
24  
25  
26  
27  
28  
29  
30  
31  
32  
33  
34  
35  
36  
37  
38  
39  
40  
41  
42  
43  
44  
45  
46  
47  
48  
49  
50  
51  
52  
53  
54  
55  
56  
57  
58  
59  
60



Figure 1. Picture of the Alpha6 Generator test site in TurboCare (Torino, Italy)

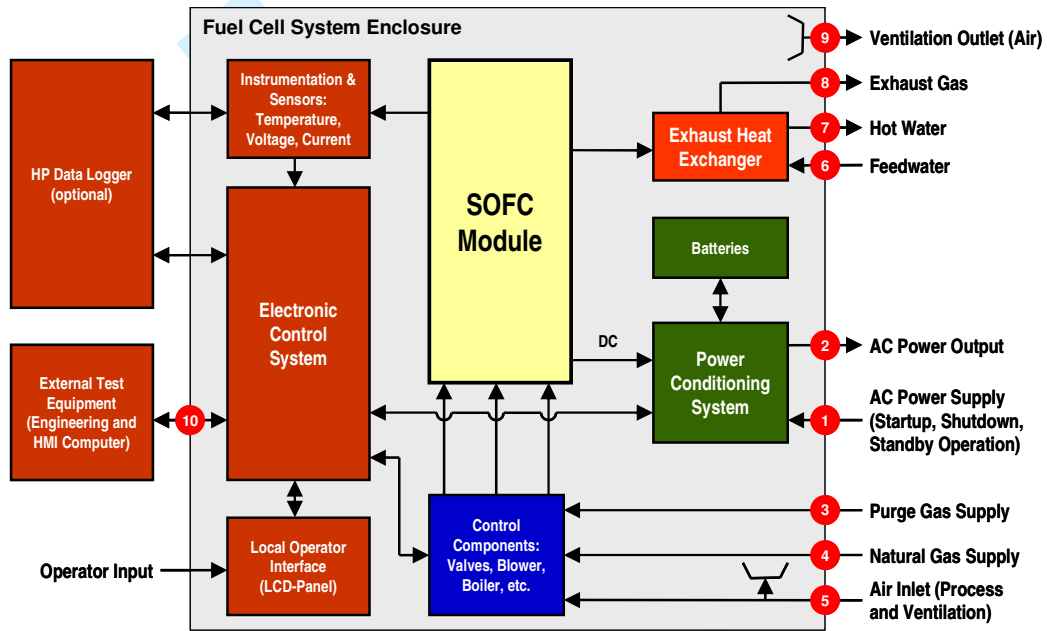


Figure 2. Simplified scheme of the Balance of Plant of the 5 kWe Alpha6 Generator

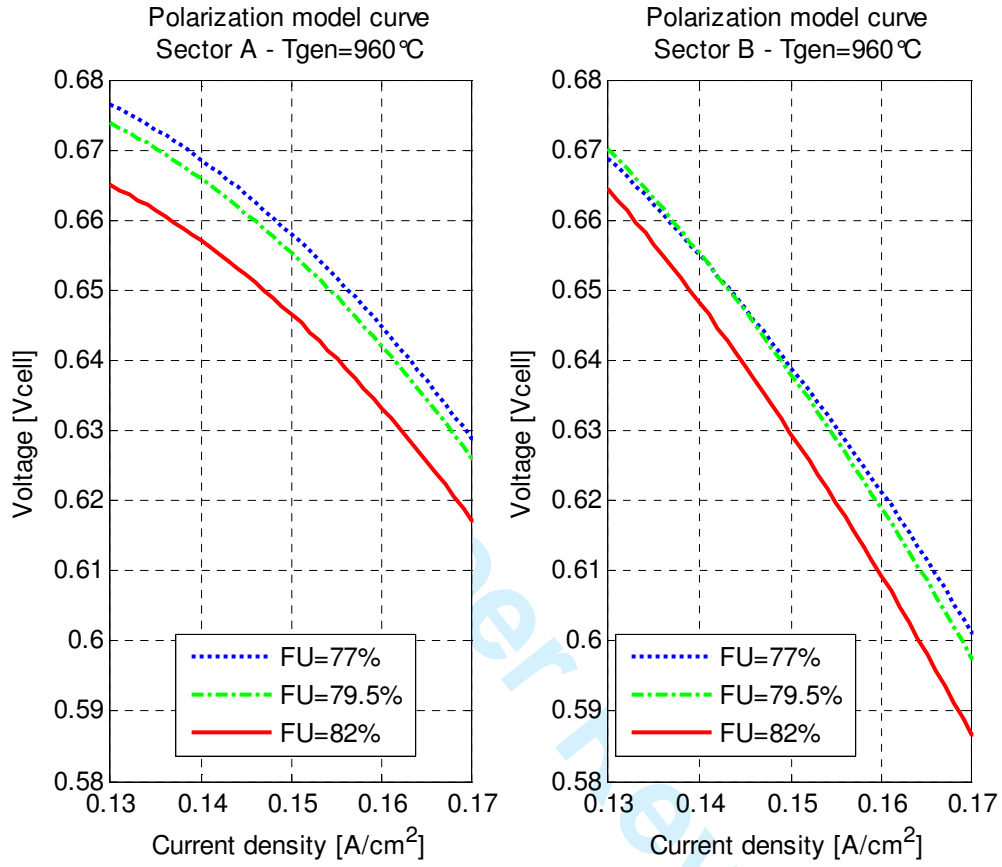


Figure 3. Polarization model for sector A and B, function of FU

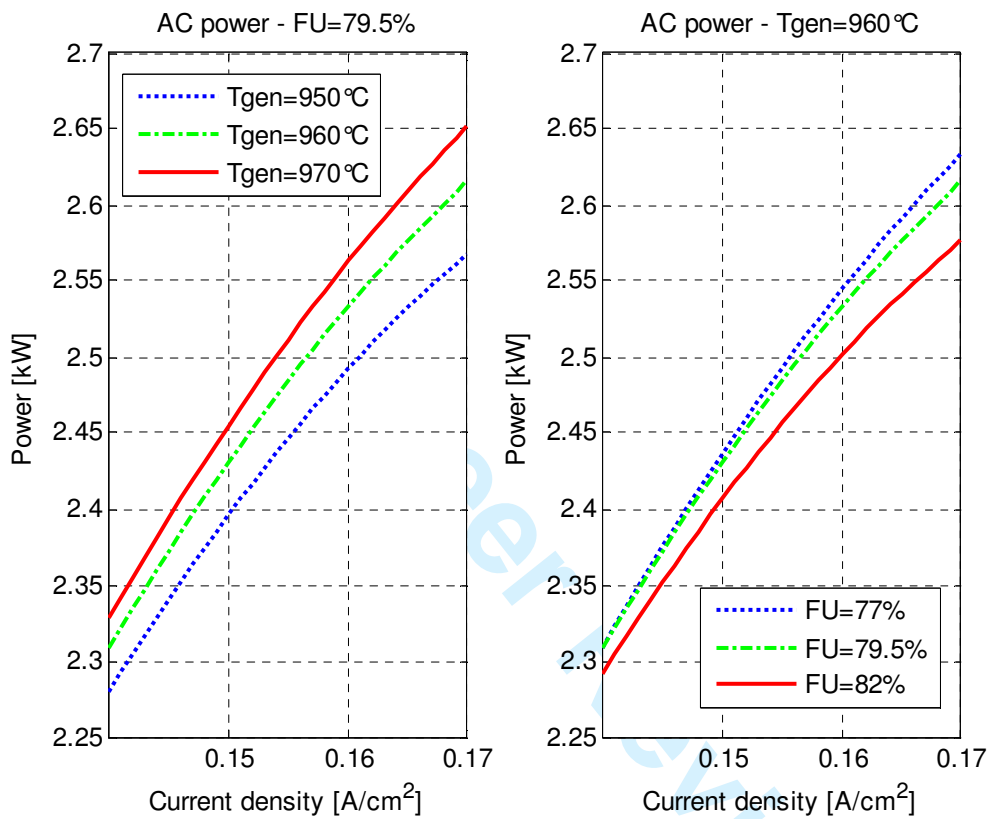


Figure 4. AC power model, function of current density, T<sub>gen</sub> and FU

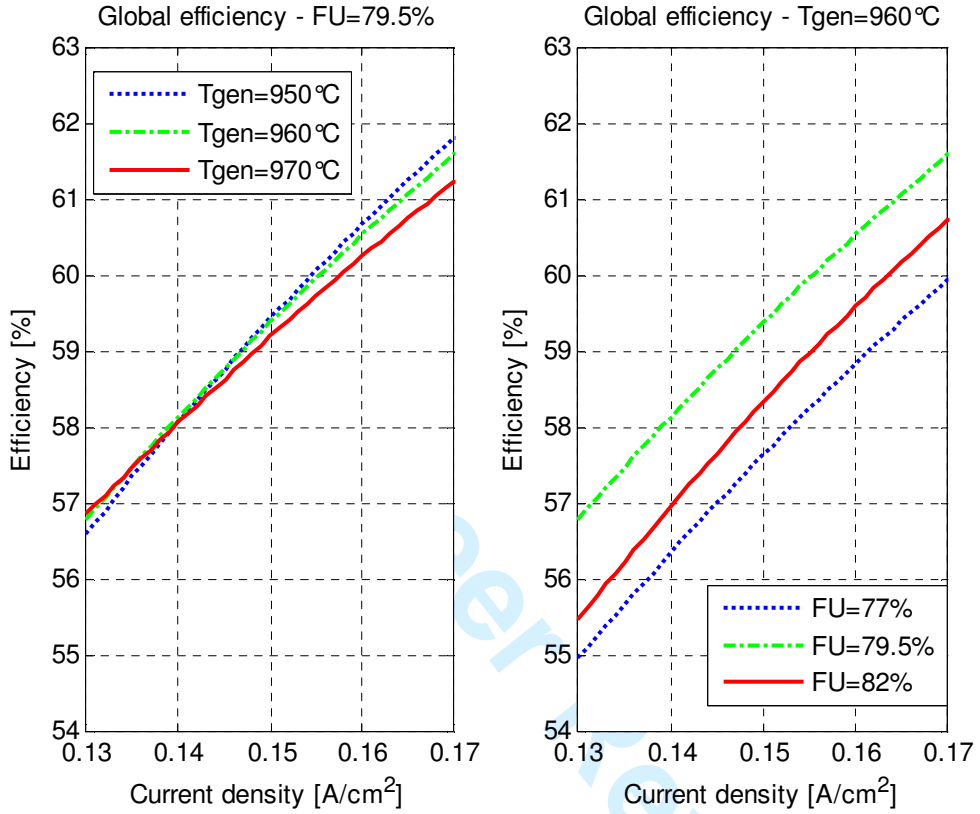


Figure 5. Global efficiency model, function of current density, T<sub>gen</sub> and FU

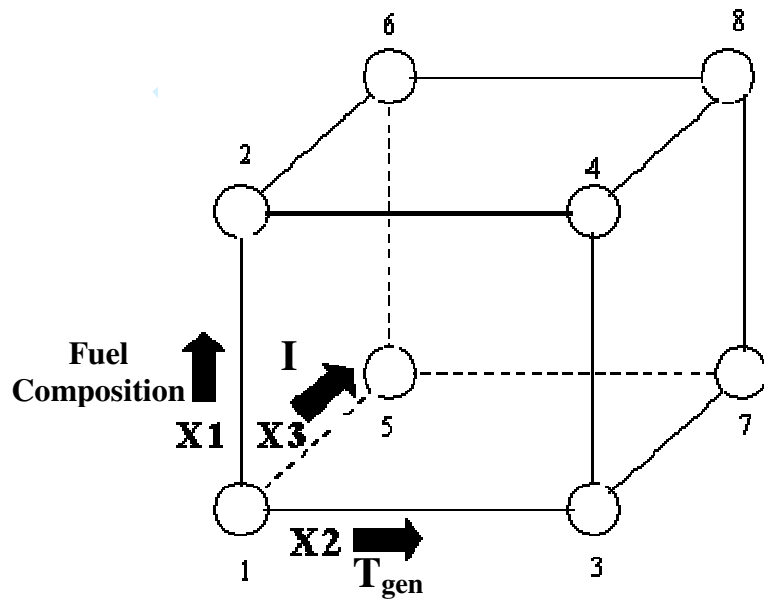


Figure 6. 2<sup>3</sup> factorial design

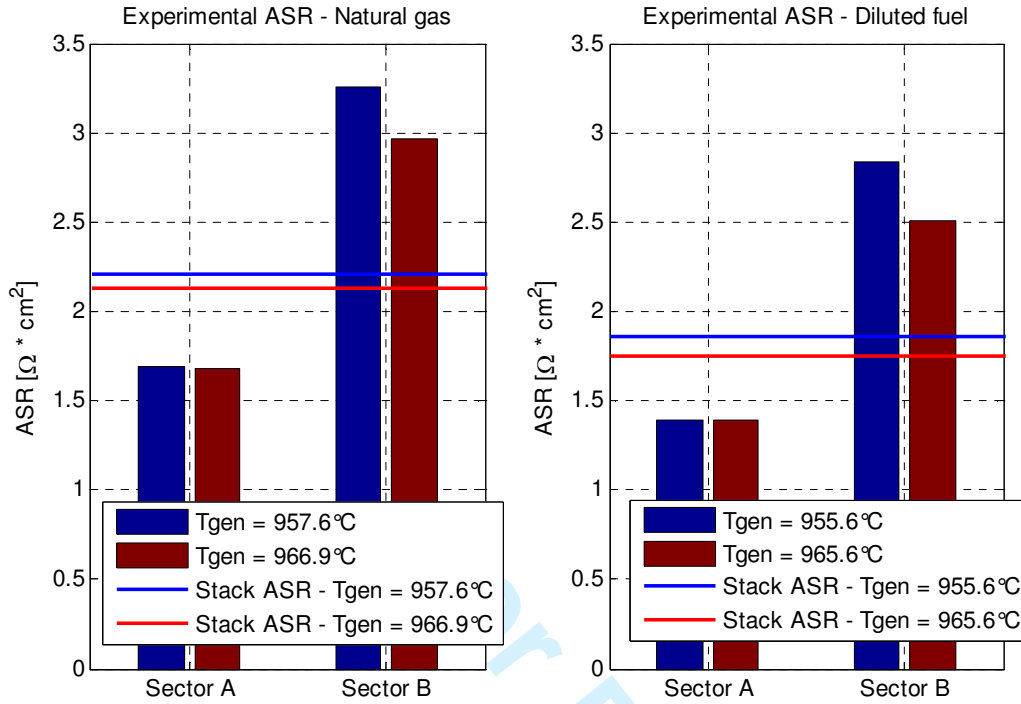


Figure 7. ASR distribution function of fuel composition and generator average temperature

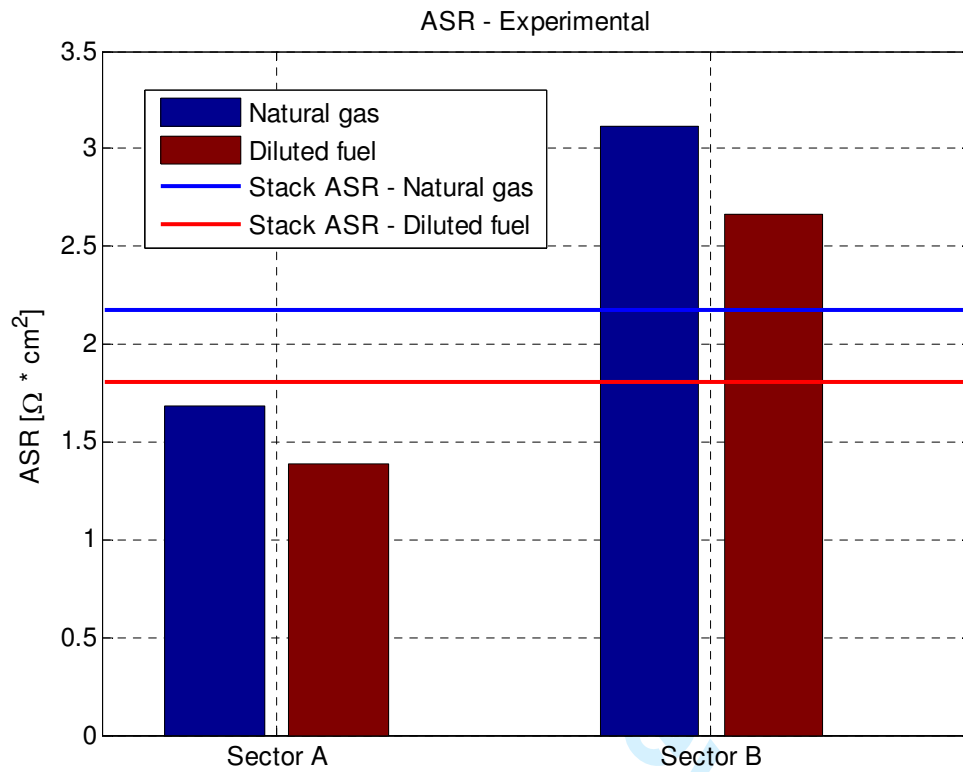


Figure 8. ASR function of the fuel composition

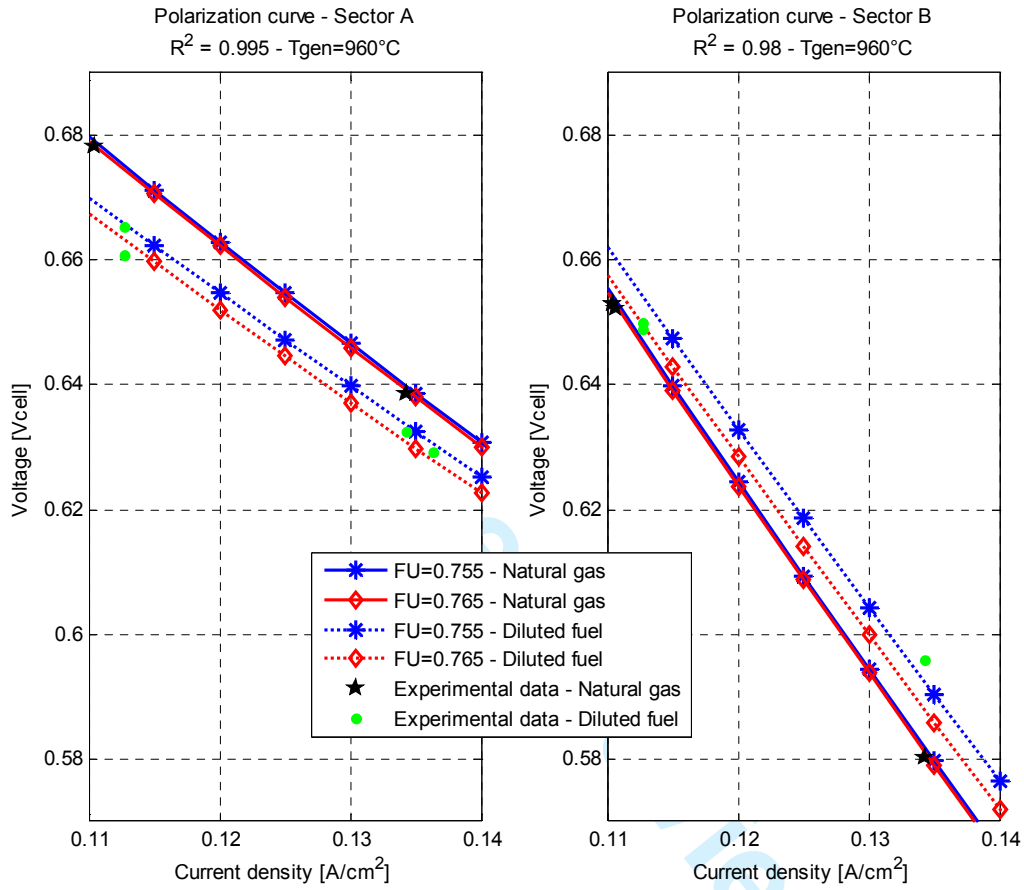


Figure 9. Polarization regression model function of current density, FU and fuel composition

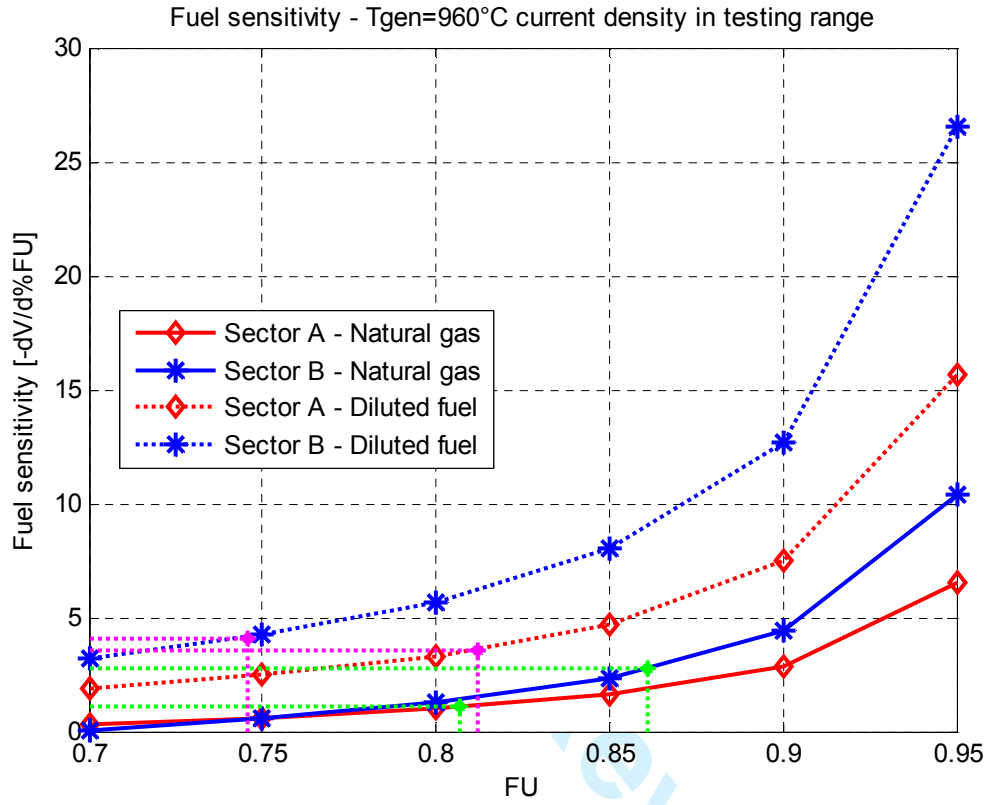


Figure 10. Estimation of local values of fuel utilization through analysis of voltage sensitivity to fuel utilization